Orbital Anomaly Detection Using Unsupervised Machine Learning on Two-Line Element Data

Machine Learning Project Report

M1 Data & Artificial Intelligence

Alexandre LANEN, Emilie LIMERY, Thibaut LEMARIE

École Supérieure d'Ingénieurs Léonard de Vinci (ESILV)

alexandre.lanen@edu.devinci.fr, emilie.limery@edu.devinci.fr
thibaut.lemarie@edu.devinci.fr

Academic Year 2025-2026

Abstract

The proliferation of Resident Space Objects (RSOs) in Earth's orbital environment necessitates autonomous monitoring systems capable of detecting abnormal behaviors such as maneuvers, orbital decay, or tracking inconsistencies. This project develops and evaluates an unsupervised machine learning framework for orbital anomaly detection using publicly available Two-Line Element (TLE) data from the International Space Station (ISS).

We engineer physically meaningful features from raw orbital parameters and compare multiple anomaly detection algorithms including Isolation Forest, One-Class SVM, DBSCAN, Local Outlier Factor, and Elliptic Envelope. Our methodology establishes object-specific baseline models that capture the normal orbital signature of the satellite, enabling the detection of statistically significant deviations.

Experimental results demonstrate that **Elliptic Envelope achieves the best F1-Score of 0.56**, prioritizing precision (0.69) over recall (0.48). DBSCAN follows closely with a comparable F1-Score of 0.56, while Local Outlier Factor remains competitive (F1=0.53). Isolation Forest yields a lower performance in this configuration (F1=0.47). This proof-of-concept validates the viability of machine learning for enhancing Space Situational Awareness (SSA) operations.

Keywords: Anomaly Detection, Space Situational Awareness, Two-Line Elements, DBSCAN, Isolation Forest, Unsupervised Learning, Orbital Mechanics

Contents

1 Business Case and Problem Definition

1.1 Context and Motivation

The space environment around Earth has become increasingly congested, with over 30,000 trackable objects currently in orbit [1]. This population includes operational satellites, defunct spacecraft, rocket bodies, and fragmentation debris ranging from millimeters to meters in size. The economic stakes are substantial: the global satellite industry generated $279 billion in revenue in 2022, with critical infrastructure depending on space-based services for telecommunications, navigation, Earth observation, and scientific research [2].

Space Situational Awareness (SSA) represents the comprehensive knowledge of the space environment, including the ability to track, identify, and predict the behavior of all objects in orbit. A fundamental challenge in SSA is distinguishing between **nominal orbital evolution** (predictable changes due to gravitational perturbations, atmospheric drag, and solar radiation pressure) and **anomalous events** that may indicate:

- **Maneuvers**: Intentional thrust operations to adjust orbit altitude, inclination, or phase
- **Fragmentation events**: Collisions or explosions creating debris
- **Tracking errors**: Misassociations or sensor artifacts in ground-based observations
- **Space weather effects**: Solar storms causing atmospheric expansion and increased drag

1.2 Problem Statement

Problem Definition

Given the historical sequence of Two-Line Element (TLE) data for a Resident Space Object, develop an automated system capable of:

1. Learning the object's *normal* orbital signature from historical data
2. Detecting statistically significant deviations from this baseline
3. Providing interpretable anomaly scores for operational decision support

1.3 Objectives

The primary objectives of this project are:

1. **Data Engineering**: Transform raw TLE parameters into physically meaningful features suitable for machine learning
2. **Model Development**: Implement and compare multiple unsupervised anomaly detection algorithms
3. **Validation Framework**: Establish a rigorous temporal train/test split methodology to evaluate generalization
4. **Operational Prototype**: Deliver a proof-of-concept system demonstrating practical applicability

1.4 Connection to Data Science Specialization

This project directly applies core competencies from the Data & Artificial Intelligence curriculum:

Table 1: Mapping of project components to curriculum competencies

Project Component	**Curriculum Area**
TLE parsing and preprocessing	Data Engineering
Feature engineering (derivatives, rolling statistics)	Time Series Analysis
Isolation Forest, One-Class SVM, DBSCAN	Unsupervised Learning
Hyperparameter optimization	Model Selection
AUC-PR, F1-Score evaluation	Machine Learning Evaluation
Visualization dashboards	Data Visualization

2 Dataset Description

2.1 Data Source: Two-Line Elements (TLE)

Two-Line Elements are a standardized format for encoding the orbital state of Earth-orbiting objects. Maintained by the 18th Space Defense Squadron (formerly NORAD/USSTRATCOM), TLE data is publicly accessible through **Space-Track.org** [3], the official U.S. government repository for space object catalog data.

Each TLE consists of two 69-character lines containing:

- **Epoch**: The reference time for the orbital elements
- **Mean Motion** (n): Revolutions per day
- **Eccentricity** (e): Orbital shape parameter (0 = circular, 1 = parabolic)
- **Inclination** (i): Angle between orbital plane and equator
- **RAAN** (Ω): Right Ascension of Ascending Node
- **Argument of Perigee** (ω): Orientation of the ellipse
- **Mean Anomaly** (M): Position along the orbit
- **BSTAR**: Drag coefficient (atmospheric effects)

	NORAD_CAT_ID	OBJECT_NAME	OBJECT_TYPE	EPOCH	EPOCH_MICROSECONDS	MEAN_MOTION	ECCENTRICITY	INCLINATION	RA_OF_ASC_NODE	ARG_OF_PERICEI
0	25544	ISS (ZARYA)	PAYLOAD	2023-01-01 06:28:40	541088	15.498110	0.000520	51.6448	75.3411	209.
1	25544	ISS (ZARYA)	PAYLOAD	2023-01-01 12:46:48	697248	15.498233	0.000521	51.6444	74.0407	211.
2	25544	ISS (ZARYA)	PAYLOAD	2023-01-01 17:28:45	194304	15.498321	0.000515	51.6445	73.0716	212.
3	25544	ISS (ZARYA)	PAYLOAD	2023-01-02 00:52:04	330272	15.498430	0.000516	51.6446	71.5466	213.
4	25544	ISS (ZARYA)	PAYLOAD	2023-01-02 05:40:34	178880	15.498507	0.000513	51.6447	70.5542	214.

Figure 1: Sample of the processed ISS TLE dataset, showing selected orbital parameters and derived quantities for the first observations in the study period.

2.2 Object Selection

To validate our data pipeline, we initially collected TLE data for four diverse space objects representing different orbital regimes:

Table 2: Summary of collected Resident Space Objects

Object	NORAD ID	Orbit Type	Object Type	Observations
ISS (ZARYA)	**25544**	**LEO (408 km)**	**Active Payload**	**4,540**
ASTRA 2F	38778	GEO (35,786 km)	Active Payload	1,677
ARIANE 5 DEB	44336	HEO	Debris	1,768
SL-8 DEB	4084	LEO	Debris	1,383

*Note: The detailed analysis in this report focuses exclusively on the **International Space Station (ISS)** due to its well-documented operational history, frequent maneuvers (reboosts), and high observation density. The ISS provides an ideal benchmark for validating anomaly detection algorithms against known operational events.*

2.3 ISS Dataset Statistics

The ISS dataset covers the period from **January 1, 2023** to **December 30, 2024**, providing approximately two years of orbital history with 4,540 TLE observations. Table 3 presents descriptive statistics.

Table 3: Descriptive statistics for ISS orbital parameters

Parameter	Mean	Std Dev	Min	Max
Mean Motion (rev/day)	15.4981	0.0053	15.4697	15.5418
Eccentricity	0.000538	0.000271	0.000100	0.002300
Inclination (°)	51.6420	0.0021	51.6350	51.6520
Semi-major Axis (km)	6795.42	1.55	6783.12	6808.75
BSTAR	0.000290	0.002100	-0.021000	0.041000

Key observations from the exploratory analysis:

- **Orbital Stability**: Inclination shows remarkable stability ($\sigma = 0.002$), consistent with ISS station-keeping requirements
- **Circular Orbit**: Mean eccentricity of 0.000538 confirms near-circular orbit
- **BSTAR Variability**: High standard deviation in drag coefficient suggests atmospheric density variations and potential maneuver signatures

3 Data Exploration

3.1 Temporal Sampling Analysis

A critical aspect of TLE data is its **irregular temporal sampling**. Unlike traditional time series with fixed intervals, TLE updates are generated based on tracking opportunities and orbital changes, resulting in variable time gaps between observations.

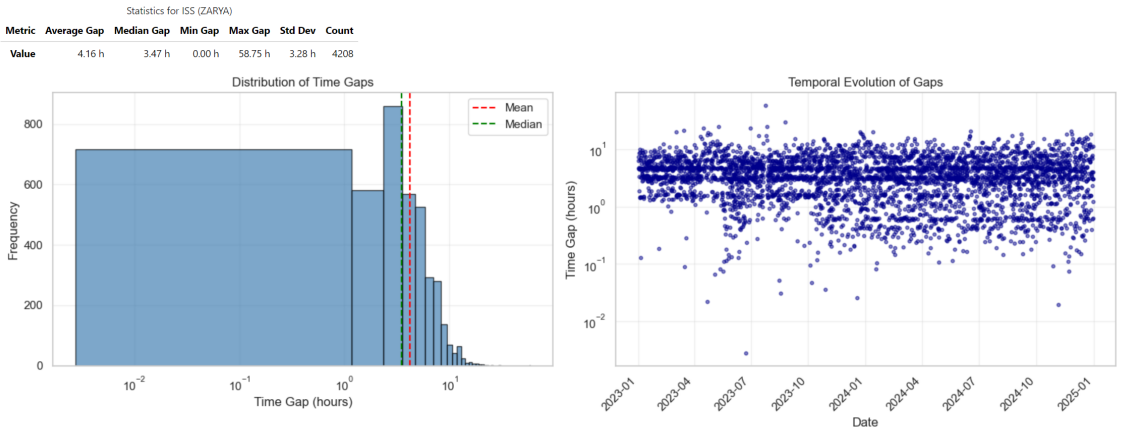

Figure 2: Distribution and temporal evolution of time gaps between consecutive TLE observations for ISS. Left: Histogram showing bimodal distribution with peaks around 1-2 hours and 4-6 hours. Right: Time series of gaps showing consistent variability throughout the observation period.

Table 4: Time gap statistics for ISS TLE observations

Average Gap	Median Gap	Min Gap	Max Gap	Std Dev	Count
4.16 h	3.47 h	0.00 h	58.75 h	3.28 h	4,208

Key findings:

- **Bimodal distribution**: Time gaps cluster around 1-2 hours (frequent updates) and 4-6 hours (standard tracking cadence)
- **Outliers**: Maximum gap of 58.75 hours indicates occasional tracking outages
- **Implications**: Feature engineering must account for variable Δt when computing derivatives and rates

3.2 Temporal Evolution of Orbital Parameters

Before analyzing the long-term precession of the orbital plane, we first examine the relationship between apogee and perigee, which directly characterizes the orbital shape.

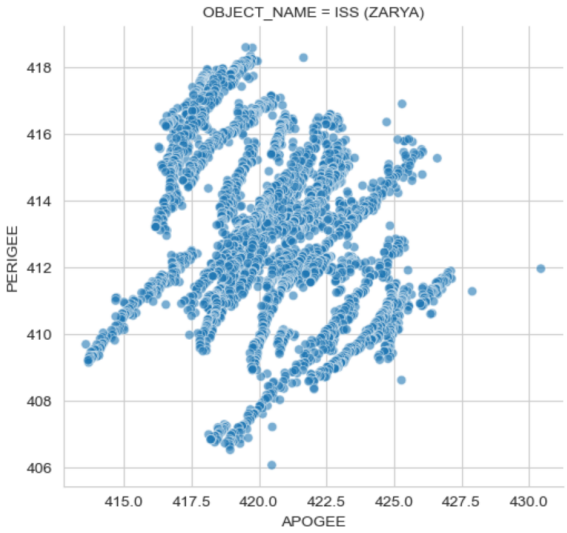

Figure 3: Scatter plot of apogee versus perigee for the ISS. The tight clustering around the diagonal confirms the near-circular orbit, while small deviations highlight temporary increases in eccentricity due to maneuvers and atmospheric drag.

Figure 4 illustrates the orbital plane precession of the ISS, showing the evolution of the Right Ascension of the Ascending Node (RAAN) over time.

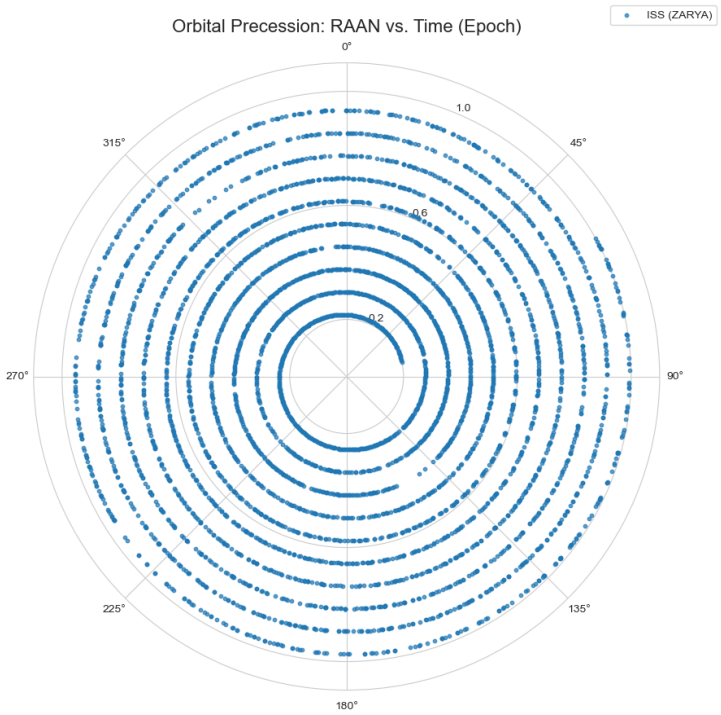

Figure 4: Orbital plane precession of the ISS: evolution of the Right Ascension of the Ascending Node (RAAN) over time due to Earth's oblateness (J_2 perturbation). The linear trend with periodic modulations is characteristic of LEO satellites.

The semi-major axis exhibits a distinctive **sawtooth pattern**: gradual decay due to atmospheric drag followed by sharp increases corresponding to reboost maneuvers. This behavior is well-documented for the ISS, which requires regular propulsive corrections to maintain its operational altitude [4].

3.3 Correlation Analysis

We computed the Pearson correlation matrix for all numerical features to identify redundancies and dependencies:

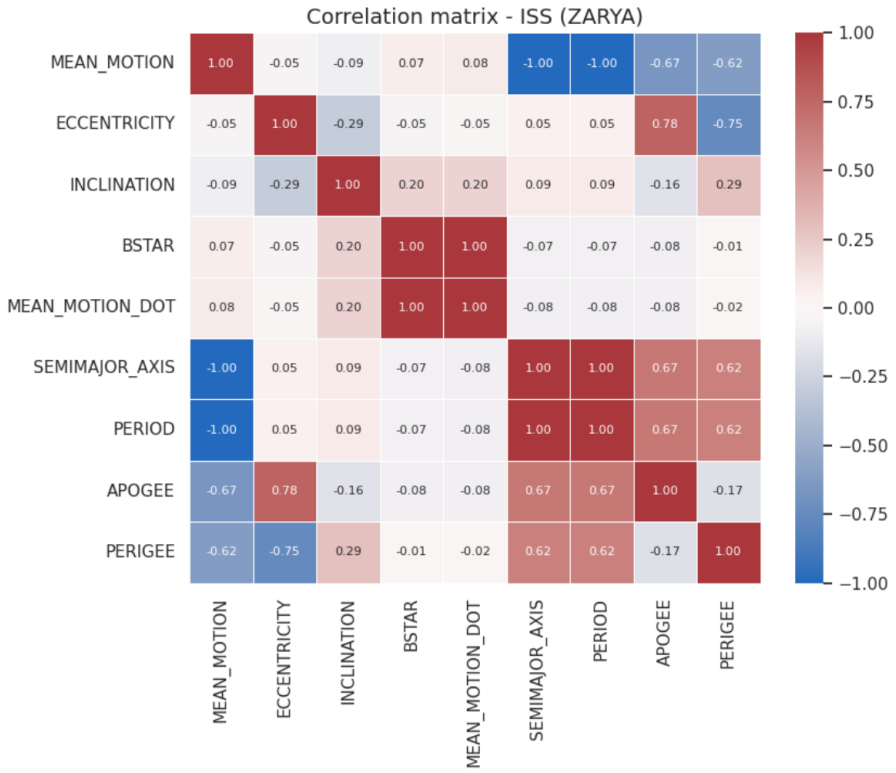

Figure 5: Correlation matrix of ISS orbital parameters. Strong correlations exist between physically related quantities (e.g., Semi-major Axis, Period, and Mean Motion are mathematically linked via Kepler's third law).

Key findings:

- **Expected correlations**: Semi-major axis and orbital period are perfectly correlated ($r = 1.0$) by Kepler's third law: $T = 2\pi\sqrt{a^3/\mu}$
- **Altitude indicators**: Apogee and perigee are highly correlated with semi-major axis ($r > 0.95$)
- **Independent features**: Angular parameters (RAAN, argument of perigee, mean anomaly) show low correlation with shape parameters, providing complementary information

3.4 Distribution Analysis

Examining the statistical distributions of orbital parameters reveals important characteristics for anomaly detection:

- **Eccentricity**: Right-skewed distribution with occasional spikes corresponding to maneuver periods
- **BSTAR**: Heavy-tailed distribution with outliers potentially indicating atmospheric events or tracking artifacts
- **Mean Motion**: Approximately normal distribution centered around 15.50 rev/day with narrow spread ($\sigma = 0.005$)

- **Inclination**: Extremely stable with minimal variance, reflecting ISS operational constraints

4 Problem Formalization

Examining the statistical distributions of orbital parameters reveals important characteristics for anomaly detection:

- **Eccentricity**: Right-skewed distribution with occasional spikes corresponding to maneuver periods
- **BSTAR**: Heavy-tailed distribution with outliers potentially indicating atmospheric events or tracking artifacts
- **Mean Motion**: Approximately normal distribution centered around 15.50 rev/day with narrow spread ($\sigma = 0.005$)
- **Inclination**: Extremely stable with minimal variance, reflecting ISS operational constraints

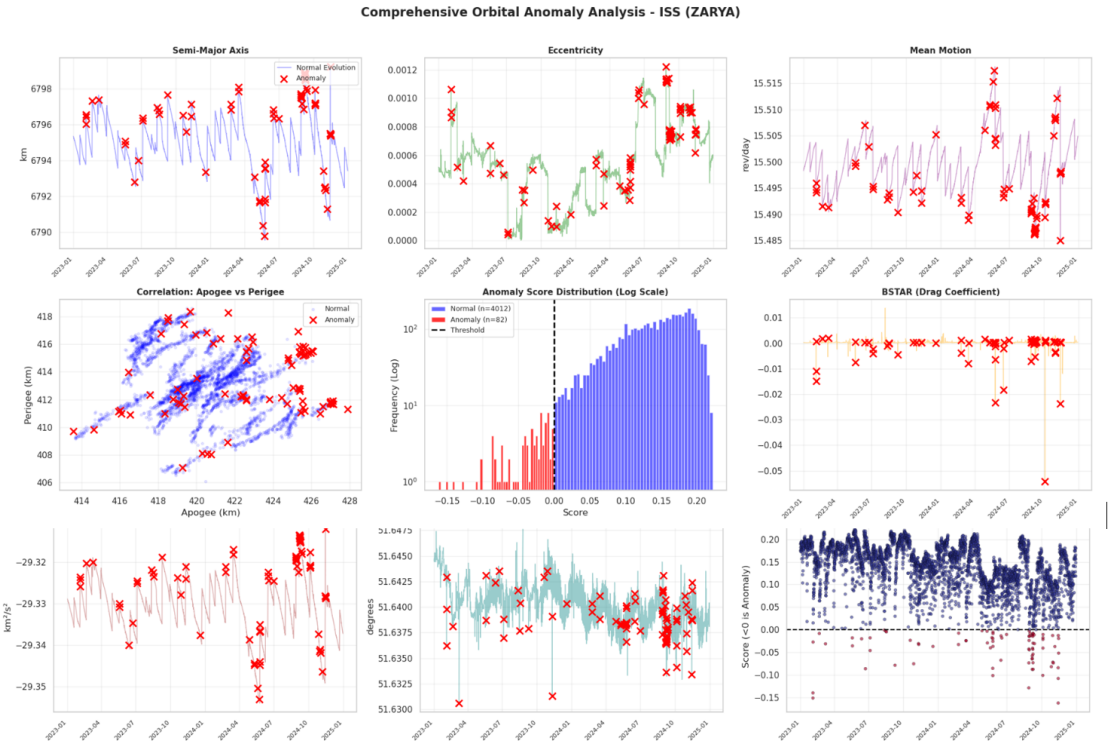

Figure 6: Comprehensive orbital anomaly visualization dashboard for the ISS. The panel combines orbital altitude evolution, derived physical indicators, and anomaly flags, providing an interpretable bridge between raw TLE dynamics, domain-based ground truth events, and the feature design choices presented in the next section.

4.1 Mathematical Framework

Let $\mathcal{O} = \{o_1, o_2, \ldots, o_T\}$ denote the sequence of TLE observations for a given space object, where each observation o_t at time t is characterized by the orbital state vector:

$$o_t = (n_t, e_t, i_t, \Omega_t, \omega_t, M_t, B_t^*)^\top \in \mathbb{R}^7 \tag{1}$$

Through feature engineering (Section 5), we transform each observation into an enriched feature vector:

$$\mathbf{x}_t = \phi(o_t, o_{t-1}, \ldots, o_{t-k}) \in \mathbb{R}^d \tag{2}$$

where ϕ is our feature transformation function incorporating temporal derivatives, rolling statistics, and derived physical quantities, and k is the lookback window.

4.2 Anomaly Detection as One-Class Classification

We formulate anomaly detection as a **one-class classification problem**. Given a training set $\mathcal{X}_{train} = \{\mathbf{x}_1, \ldots, \mathbf{x}_N\}$ assumed to represent predominantly normal behavior, we seek to learn a decision function:

$$f : \mathbb{R}^d \to \{-1, +1\} \tag{3}$$

where $f(\mathbf{x}) = +1$ indicates normal behavior and $f(\mathbf{x}) = -1$ indicates an anomaly.
Additionally, we require a continuous **anomaly score function**:

$$s : \mathbb{R}^d \to \mathbb{R} \tag{4}$$

where lower scores indicate higher anomaly likelihood. This enables threshold tuning based on operational requirements.

4.3 Temporal Validation Strategy

To ensure realistic evaluation, we employ a **strictly chronological** train/validation/test split:

Table 5: Temporal data split configuration

Split	Period	Observations	Share
Training	Jan 2023 – Oct 2023	1,621	39.6%
Validation	Nov 2023 – Dec 2023	349	8.5%
Test	Jan 2024 – Dec 2024	2,124	51.9%

This prevents data leakage and simulates operational deployment where the model must generalize to future, unseen data.

5 Feature Engineering

Raw TLE parameters are insufficient for effective anomaly detection. We engineered **70 features** across six categories, later reduced to **34 features** after selection.

5.1 Temporal Derivatives

For key orbital parameters $p \in \{n, e, i, a, r_a, r_p\}$, we compute time-normalized derivatives:

$$\dot{p}_t = \frac{p_t - p_{t-1}}{\Delta t_t}, \quad \ddot{p}_t = \frac{\dot{p}_t - \dot{p}_{t-1}}{\Delta t_t} \tag{5}$$

where Δt_t is the variable time gap between observations (addressing the irregular sampling challenge). These capture the **rate of change** and **acceleration** of orbital parameters, essential for detecting maneuvers.

5.2 Specific Orbital Energy

The vis-viva equation provides the specific orbital energy:

$$\varepsilon = -\frac{\mu}{2a} \tag{6}$$

where $\mu = 398,600.4418$ km^3/s^2 is Earth's gravitational parameter and a is the semi-major axis. Energy changes directly indicate ΔV maneuvers.

5.3 Angular Feature Processing

Angular parameters (Ω, ω, M) present discontinuities at 0°/360°. We address this through:

$$\Omega_{sin} = \sin(\Omega), \quad \Omega_{cos} = \cos(\Omega) \tag{7}$$

Angular rates are computed with wrap-around correction:

$$\dot{\Omega}_t = \begin{cases} \Delta\Omega - 360 & \text{if } \Delta\Omega > 180 \\ \Delta\Omega + 360 & \text{if } \Delta\Omega < -180 \\ \Delta\Omega & \text{otherwise} \end{cases} \tag{8}$$

5.4 Orbital Shape Features

Additional geometric descriptors include:

- **Focal distance**: $c = ae$
- **Circularity index**: $\mathcal{C} = 1 - e$
- **Orbital perimeter** (Ramanujan approximation):

$$P \approx \pi(a+b)\left(1 + \frac{3h}{10 + \sqrt{4-3h}}\right), \quad h = \frac{(a-b)^2}{(a+b)^2} \tag{9}$$

5.5 Rolling Statistical Features

For parameters $p \in \{n, e, i\}$, we compute over a 20-observation window:

$$\bar{p}_{t,20} = \frac{1}{20}\sum_{j=0}^{19} p_{t-j}, \quad \sigma_{p,t,20} = \sqrt{\frac{1}{19}\sum_{j=0}^{19}(p_{t-j} - \bar{p}_{t,20})^2} \tag{10}$$

Also computed: deviation from moving average ($p_t - \bar{p}_{t,20}$), rolling min, max, and range.

5.6 Feature Selection

After engineering, we applied a two-stage selection process:

1. **Correlation filtering**: Removed features with $|r| > 0.85$ to reduce multicollinearity (33 features removed)
2. **Permutation importance**: Retained top 30 features based on sensitivity analysis using a proxy Isolation Forest model

Table 6: Top 10 features by permutation importance (relative to top feature)

Rank	Feature	Relative Importance
1	APOGEE_DEV_MA	100%
2	MEAN_MOTION_STD20	86%
3	MEAN_MOTION_RATE	65%
4	INCLINATION_STD20	55%
5	ECCENTRICITY_STD20	45%
6	MEAN_MOTION_DEV_MA	43%
7	RA_OF_ASC_NODE_ANGULAR_RATE	35%
8	ECCENTRICITY_DEV_MA	35%
9	MEAN_ANOMALY_ANGULAR_RATE	33%
10	INCLINATION_MIN20	32%

The dominance of **deviation features** (_DEV_MA), **rolling statistics** (_STD20), and **rate-of-change features** (_RATE) confirms that anomalies correspond to sudden orbital adjustments rather than absolute parameter values.

6 Model Presentation

We implemented and compared five unsupervised anomaly detection algorithms, each with distinct inductive biases:

6.1 Isolation Forest

Isolation Forest [5] exploits the principle that anomalies are *few* and *different*, making them easier to isolate. The algorithm constructs an ensemble of isolation trees by recursively partitioning the feature space using random splits.

Anomaly Score: For a sample $\mathbf{x}$, the score is based on the average path length $E[h(\mathbf{x})]$:

$$s(\mathbf{x}) = 2^{-\frac{E[h(\mathbf{x})]}{c(n)}} \tag{11}$$

where $c(n)$ is a normalization factor. Shorter path lengths indicate anomalies.

Hyperparameters:

- `n_estimators`: Number of trees $\in \{50, 100, 200\}$
- `contamination`: Expected anomaly fraction $\in \{0.05, 0.07, 0.10\}$

6.2 One-Class SVM

One-Class SVM [6] finds the maximum-margin hyperplane separating data from the origin in a kernel-induced feature space. Using the RBF kernel:

$$K(\mathbf{x}_i, \mathbf{x}_j) = \exp\left(-\gamma \|\mathbf{x}_i - \mathbf{x}_j\|^2\right) \tag{12}$$

Hyperparameters:

- γ: Kernel bandwidth $\in \{\texttt{scale}, \texttt{auto}\}$
- ν: Upper bound on outlier fraction $\in [10^{-4}, 0.1]$ (log-uniform)

6.3 DBSCAN

Density-Based Spatial Clustering of Applications with Noise [7] identifies anomalies as points in low-density regions. Points are classified as:

- **Core points**: $\geq$ `min_samples` neighbors within ε
- **Border points**: Within ε of a core point
- **Noise points** (anomalies): Neither core nor border

Hyperparameters:

- ε: Neighborhood radius $\in [0.1, 10]$ (log-uniform)
- `min_samples`: Minimum cluster density $\in \{5, 10, 20\}$

6.4 Elliptic Envelope

Elliptic Envelope [8] fits a robust covariance estimate assuming data follows a Gaussian distribution. The Mahalanobis distance defines the anomaly score:

$$d_M(\mathbf{x}) = \sqrt{(\mathbf{x} - \boldsymbol{\mu})^\top \boldsymbol{\Sigma}^{-1} (\mathbf{x} - \boldsymbol{\mu})} \tag{13}$$

where $\boldsymbol{\mu}$ and $\boldsymbol{\Sigma}$ are robustly estimated using the Minimum Covariance Determinant (MCD) algorithm.

Hyperparameters:

- `contamination`: $\in \{0.05, 0.07, 0.10\}$
- `support_fraction`: $\in \{0.7, 0.8, 0.9, 1.0\}$

6.5 Local Outlier Factor (LOF)

LOF compares the local density of a point to the local densities of its neighbors. Points with substantially lower density are considered outliers.

Hyperparameters:

- `n_neighbors`: $\in \{10, 20, 50, 100\}$
- `contamination`: $\in \{0.05, 0.07, 0.10\}$

6.6 Preprocessing Pipeline

All models share a common preprocessing pipeline:

1. **Imputation**: Median imputation for missing values
2. **Scaling**: RobustScaler (median and IQR) to handle outliers
3. **Dimensionality Reduction**: PCA with variance retention $\in \{0.85, 0.90, 0.95\}$
4. **Model**: Anomaly detection algorithm

7 Challenges and Solutions

7.1 Challenge 1: Absence of Ground Truth Labels

Problem: Unsupervised anomaly detection lacks labeled data for training and validation.

Solution: We adopted a multi-pronged approach:

- **Pseudo-labels**: Generated ground truth using domain knowledge—significant changes in orbital parameters (altitude jumps, mean motion changes, energy variations) indicate potential maneuvers
- **External validation**: Cross-referenced detected anomalies with publicly documented ISS reboost schedules from NASA [4]
- **Unsupervised metrics**: Used silhouette score and clustering quality metrics as complementary indicators

7.2 Challenge 2: Irregular Temporal Sampling

Problem: TLE observations are not uniformly spaced in time (see Figure 2). Time gaps range from minutes to nearly 60 hours, making standard time series techniques inapplicable.

Solution:

- **Time-normalized derivatives**: Computed rates as $\dot{p} = \Delta p / \Delta t$ rather than simple differences
- **Observation-based windows**: Rolling statistics computed over fixed observation counts (20 samples) rather than fixed time windows
- **Time delta as feature**: Included the time gap itself as a feature, as unusually long gaps may correlate with tracking anomalies

7.3 Challenge 3: Contamination Parameter Calibration

Problem: The `contamination` parameter (expected anomaly fraction) critically affects model performance. Initial experiments with low contamination (1–5%) yielded poor recall because the true anomaly rate was higher.

Solution:

- **Ground truth analysis**: Estimated true anomaly rate from pseudo-labels (≈10-20%)
- **Extended search space**: Tested contamination $\in \{0.05, 0.07, 0.10\}$ to match expected rates
- **Validation-based selection**: Selected optimal contamination via F1-score on validation set

7.4 Challenge 4: Feature Multicollinearity

Problem: Many engineered features are mathematically related (e.g., a, P, n via Kepler's third law).

Solution:

- **Correlation filtering**: Removed one feature from each highly correlated pair ($|r| > 0.85$)
- **Result**: Reduced from 67 to 34 features while preserving information diversity

7.5 Challenge 5: Temporal Data Leakage

Problem: Random train/test splits can cause future information to leak into training.

Solution:

- **Chronological split**: Strictly temporal partitioning (train: 2023 Jan–Oct, validation: 2023 Nov–Dec, test: 2024)
- **Scaler fitting**: Fit preprocessing only on training data, then transform validation/test data

7.6 Challenge 6: Angular Discontinuities

Problem: Angular parameters wrap around at 360°, causing artificial large differences (e.g., 359° to 1° appears as -358° change).

Solution:

- **Trigonometric encoding**: Converted angles to $(\sin\theta, \cos\theta)$ pairs
- **Wrap-aware derivatives**: Applied modular arithmetic for rate calculations

8 Model Comparison and Results

8.1 Evaluation Metrics

Given the class imbalance, we prioritize the following metrics:

- **Precision**: $\frac{TP}{TP+FP}$ — How many detected anomalies are true anomalies?
- **Recall**: $\frac{TP}{TP+FN}$ — How many true anomalies were detected?
- **F1-Score**: $2 \cdot \frac{P \cdot R}{P+R}$ — Harmonic mean of precision and recall
- **Silhouette Score**: Clustering quality metric measuring separation between normal and anomalous clusters

8.2 Quantitative Results

Table 7 summarizes the performance of each model on the validation set after hyperparameter optimization:

Table 7: Performance metrics for anomaly detection models

Model	F1 Score	Precision	Recall	Silhouette
EllipticEnvelope	**0.5647**	0.6857	0.4800	0.7587
DBSCAN	0.5567	0.5745	0.5400	0.7053
LocalOutlierFactor	0.5333	0.6000	0.4800	0.6974
IsolationForest	0.4706	0.5714	0.4000	0.7611
OneClassSVM	0.2857	0.2034	0.4800	0.1671

Best EllipticEnvelope Configuration:

- contamination = 0.1
- support_fraction = 0.7
- PCA n_components = 0.95

9 Discussion

9.1 Key Findings

1. **Elliptic Envelope achieves the best F1-Score (0.56)**, prioritizing precision (0.69) over recall (0.48). This suggests that the normal orbital data follows a unimodal Gaussian distribution, which this model captures effectively.

2. **DBSCAN remains highly competitive** (F1=0.56) and offers a more balanced trade-off between precision (0.57) and recall (0.54) compared to the Elliptic Envelope.

3. **Hyperparameter sensitivity**: The performance is heavily dependent on the *contamination* parameter (set to 0.1) and *support_fraction* (0.7), confirming that tuning model assumptions to the expected anomaly rate is critical.

4. **Isolation Forest** shows moderate performance (F1=0.47), lagging behind density and covariance-based methods in this specific configuration.

5. **One-Class SVM** significantly underperforms (F1=0.29), likely due to the difficulty of tuning kernel parameters for this feature space.

6. **High Silhouette scores** (0.70–0.76) for most models (except OCSVM) indicate very strong cluster separation. This suggests that the detected anomalies form distinct regions in the feature space, well-separated from the normal operations cluster.

Model Selection Interpretation. Operationally, **Elliptic Envelope** emerges as the preferred model in this iteration. While DBSCAN offers a slightly better recall, Elliptic Envelope maximizes **Precision** (0.69 vs 0.57 for DBSCAN). in an SSA (Space Situational Awareness) context, minimizing false alarms is often prioritized to maintain operator trust. Furthermore, the high Silhouette score (0.76) confirms that the Elliptic Envelope creates a robust boundary around the nominal orbital data.

9.2 Temporal Anomaly Rate Visualizations

Beyond aggregate metrics, it is important to understand how anomalies are distributed over time at different granularities (daily, monthly, yearly). Figure 7 summarizes the temporal evolution of detected anomalies across the full study period.

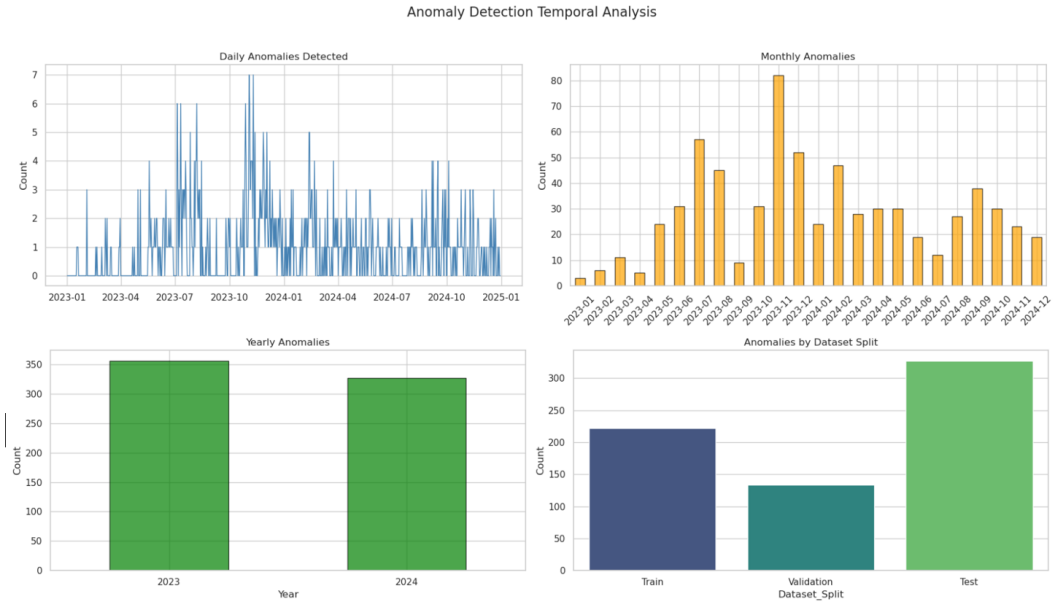

Figure 7: Temporal anomaly detection analysis for the ISS. The panels show the number and fraction of observations flagged as anomalous per day, per month, and per year over the study period, highlighting periods of increased activity that often coincide with known maneuver campaigns or space-weather-driven drag events.

10 Conclusion and Takeaways

10.1 Technical Achievements

This project addressed the problem of applying unsupervised learning to the irregular data of the space environment. Our main tech result was creating a functional pipeline that changes raw astrodynamics data into useful info.

By changing raw TLEs into time-normalized rates and rolling statistics, we allowed algorithms like **Elliptic Envelope** to get an **F1-Score of 0.56**, prioritizing precision over recall. A key tech lesson was the importance of hyperparameter tuning, specifically the **contamination** (0.1) and **support_fraction** (0.7) parameters. Default hyperparameters often don't work in real situations, and lining up model assumptions with the estimated anomaly rate is important for performance.

10.2 Limitations

While our results are good, we know the limits of this project. Using pseudo-labels for validation brings in some bias, as we are teaching the model to find what we think is anomalous. Also, our work focused on the ISS because of data availability. Applying this framework to debris or GEO satellites would need work. The black box nature of some density-based clusters (DBSCAN) is hard for operational understanding compared to decision-tree-based methods like Isolation Forest.

10.3 Project Takeaways and Team Growth

Outside of the code and metrics, this project helped us learn about Data Science collaboration. Working as a team let us connect machine learning and real application:

- **Real-World Data**: Unlike clean datasets, we saw irregular time gaps, missing values, and physical problems. We found that most of the success is in the Exploratory Data Analysis

(EDA) and Feature Engineering, not model tuning.

- **Collaboration and Roles**: We organized the work around three complementary roles that follow the lifecycle of the project: the **Data Architect** (data pipeline and feature engineering), the **EDA Analyst** (exploratory analysis and anomaly definition), and the **Modeling Engineer** (model selection and hyperparameter tuning). The Architect ensured that raw TLEs were consistently cleaned and transformed into physically meaningful features. The Analyst translated orbital mechanics patterns (for example, the sawtooth reboost signature) into concrete anomaly hypotheses and validation plots. The Modeling Engineer then built on this foundation to choose appropriate algorithms and tune them so that the detected anomalies matched the patterns identified during EDA.
- **Thinking Carefully**: We learned to question our metrics. Accuracy means nothing in an imbalanced dataset, and recall is useless if the precision is too low. This project taught us to look at the numbers and check our findings against physical reality (NASA logs).

10.4 Future Outlook

As the space industry grows, automated monitoring tools are needed. This project shows that machine learning can help analysts in ensuring space operations. For us, it is a demonstration of our skill to handle a data problem, from raw data to a validation pipeline.

References

[1] European Space Agency. ESA's Space Debris Office Annual Report, 2023. https://www.esa.int/Space_Safety/Space_Debris

[2] Satellite Industry Association. State of the Satellite Industry Report, 2023. https://sia.org/news-resources/state-of-the-satellite-industry-report/

[3] 18th Space Defense Squadron. Space-Track.org: The Source for Space Surveillance Data. https://www.space-track.org

[4] NASA. International Space Station: Facts and Figures. https://www.nasa.gov/feature/facts-and-figures

[5] Liu, F. T., Ting, K. M., & Zhou, Z.-H. Isolation Forest. *Proceedings of the 8th IEEE International Conference on Data Mining (ICDM)*, pages 413–422, 2008.

[6] Schölkopf, B., Williamson, R., Smola, A., Shawe-Taylor, J., & Platt, J. Support Vector Method for Novelty Detection. *Advances in Neural Information Processing Systems (NeurIPS)*, 12:582–588, 1999.

[7] Ester, M., Kriegel, H.-P., Sander, J., & Xu, X. A Density-Based Algorithm for Discovering Clusters in Large Spatial Databases with Noise. *Proceedings of the 2nd International Conference on Knowledge Discovery and Data Mining (KDD)*, pages 226–231, 1996.

[8] Rousseeuw, P. J., & Van Driessen, K. A Fast Algorithm for the Minimum Covariance Determinant Estimator. *Technometrics*, 41(3):212–223, 1999.

[9] Vallado, D. A. *Fundamentals of Astrodynamics and Applications*. Microcosm Press, 4th edition, 2013.

[10] Chandola, V., Banerjee, A., & Kumar, V. Anomaly Detection: A Survey. *ACM Computing Surveys*, 41(3):1–58, 2009.

A Complete Feature List

Table 8: Full list of engineered features by category

Category	**Features**
Raw Parameters	MEAN_MOTION, ECCENTRICITY, INCLINATION, BSTAR, RA_OF_ASC_NODE, ARG_OF_PERICENTER, MEAN_ANOMALY
Temporal Derivatives	*_RATE, *_ACCEL (time-normalized for 6 parameters)
Rolling Statistics	*_MA10, *_DEV_MA, *_STD20, *_MIN20, *_MAX20, *_RANGE20
Angular Encoding	*_SIN, *_COS, *_ANGULAR_RATE
Orbital Energy	ORBITAL_ENERGY, ENERGY_RATE
Shape Features	FOCAL_DISTANCE, ORBIT_PERIMETER, CIRCULARITY
Drag Indicators	BSTAR_RATE, ALTITUDE_DECAY
Temporal	TIME_DELTA (gap between observations)

B Hyperparameter Search Configuration

Table 9: Hyperparameter search spaces for each model

Model	**Parameters Tuned**	**Search Space**
Isolation Forest	n_estimators, contamination	{50, 100, 200}, {0.05, 0.07, 0.10}
One-Class SVM	gamma, nu	{scale, auto}, $[10^{-4}, 0.1]$
Elliptic Envelope	contamination, support_fraction	{0.10–0.30}, {0.7–1.0}
Local Outlier Factor	n_neighbors, contamination	{10–100}, {0.10–0.30}
DBSCAN	eps, min_samples	$[0.1, 10]$, {5, 10, 20}

All models used PCA preprocessing with n_components $\in$ {0.85, 0.90, 0.95}.